

# TURBULENT HEAT TRANSFER IN AN ABRUPT CONTRACTION CHANNEL WITH A POROUS OBSTACLE USING A NONLINEAR MODEL WITH HIGH REYNOLDS NUMBER WALL FUNCTION

Marcelo Assato<sup>1</sup>

Marcelo J.S. De-Lemos<sup>2\*</sup>

Departamento de Energia - IEME

Instituto Tecnológico de Aeronáutica - ITA

12228-900 - São José dos Campos - SP – Brasil

E-mail: <sup>1</sup>assato@aer.ita.br, <sup>2</sup>delemos@mec.ita.br

\* Corresponding author

**Abstract:** This work presents a numerical investigation for the turbulent flow and heat transfer in an abrupt contraction channel with a porous material placed in a flow passage. The channel has a contraction rate of 3:2. Results for the hybrid medium were obtained using linear and nonlinear  $k - \epsilon$  macroscopic models. It was used an inlet Reynolds number of  $Re = 132000$  based on the height of the step. Parameters such as porosity, permeability and thickness of the porous insert were varied in order to analyze their effects on the flow pattern. The results of local heat transfer and friction coefficient obtained by the two turbulence models were compared for the cases without and with porous insertion of thickness,  $a=0.083H$ ,  $a=0.166H$  and  $a=0.250H$ , where  $H$  is the step height, porosity of 0.85 and 0.95, and permeability of  $10^{-6}$ ,  $10^{-4}$  and  $10^{-2} \text{ m}^2$ .

**Keywords.** porous obstruction, turbulent heat transfer, non-linear model, abrupt contraction channel.

## 1. INTRODUCTION

Fluid flow and forced convection heat transfer in hybrid configurations (clean and porous media) have been investigated experimentally and numerically in several works. The insertion of a porous material in a channel can improve the heat transfer and control a local flow. Flows in channels with steps, over sinusoidal surfaces or inside diffusers, are examples of configurations that appear recirculating bubbles. Sometimes the attenuation or even the suppression of the recirculating bubble is desired. The effectiveness of using a porous matrix to improve the heat transfer has been proven. However, besides the porous material to increase the transfer of heat, the pressure drop is also greatly increased. Depending on certain parameter, such as porous insert thickness, porosity and permeability, the rate of increase of the pressure drop can be far greater than that of the heat transfer coefficient. Thus, these two parameters must be analyzed and considered in the design of thermo-mechanical equipments.

Laminar or turbulent forced convection heat transfer in porous media has many practical applications such as petroleum processing, combustion in porous matrices, filtering, heat exchangers, electronic equipment cooling, soil contaminant dispersion, etc.

More recently, some problems such as: flow past a backward-facing step with porous inserts has been studied numerically by Rocamora and de Lemos (2000), Chan et al. (2000), Assato et al. (2002) and Assato and de Lemos (2003). The first two works presented laminar and turbulent results with forced convective heat transfer. They used for modeling turbulent flow a two-equation linear  $k-\epsilon$  model with wall function for both the fluid region and the porous medium. Rocamora and de Lemos (2000) treat the interface between the porous medium and the clear fluid following the work in Ochoa-Tapia and Whitaker (1995). Chan et al. (2000) considered the flow at the interface between the fluid and porous medium as being continuous. The presence of the Brinkman's extension model (Brinkman (1948)) in the porous media equation eliminates the need for imposing an explicit interface condition, in accordance with Nield and Bejan (1992). Assato et al. (2002) and Assato and de Lemos (2003) presented turbulent results using linear and non-linear eddy viscosity macroscopic models. They showed that depending of porous insert parameters is obtained a total damping of the recirculation bubble.

In present work, numerical results for turbulent flow and heat transfer in an abrupt contraction channel with a porous insert is presented. Both *linear* and *non-linear* eddy viscosity macroscopic models are employed. Here, the boundary conditions at the porous medium/clear fluid interface are the same used by Rocamora and de Lemos (2000), Assato et al. (2002) and Assato and de Lemos (2003).

The non-linear eddy viscosity models (NLEVM) which represent an extension of the LEVM have shown good performance in clean flows where the Reynolds normal stresses play an important role (Assato and de Lemos (2000)) correcting the deficiencies presented by the LEVM. They basically follow the procedures used in obtaining constitutive equations for laminar flow of non-Newtonian fluids (Rivlin (1957)). Example is the work of Speziale (1987). Essentially, the observed relationship between laminar flow of viscoelastic fluids and turbulent flow of Newtonian substances has motivated developments of such Non-Linear Models (NLEVM, Lumley (1970)). The basic advantage of the NLEVM over others more complex models, e.g. the algebraic stress model (ASM) lies on the achieved computational savings (roughly 25-50% less computing time).

Therefore, in this article comparisons of results simulated with both linear and non-linear  $k-\epsilon$  turbulence models for turbulent flow through an abrupt contraction channel with a porous obstruction placed in a flow passage are shown. Some important parameters such as porosity, permeability and thickness of the porous insert are varied and their effects on the flow and thermal fields are assessed.

## 2. MACROSCOPIC TRANSPORT EQUATIONS.

The works of Pedras and de Lemos (2001<sup>a,b,c</sup>) present the macroscopic transport equations used this study. They were developed for an incompressible fluid in a rigid, homogeneous and saturated porous medium, and for the turbulent flow regime are obtained through the application of the time and volume average operators, with the help of the Local Volume Average Theorems (LVAT) and the '*double decomposition*'. The equations system is composed by the macroscopic continuity, momentum, energy, turbulent kinetic energy, dissipation rate of turbulent kinetic energy, Reynolds stress, eddy viscosity equations.

$$\nabla \cdot \bar{\mathbf{u}}_D = 0 \quad (1)$$

$$\begin{aligned} \left[ \nabla \cdot \left( \mathbf{r} \frac{\bar{\mathbf{u}}_D \bar{\mathbf{u}}_D}{\mathbf{f}} \right) \right] &= -\nabla \cdot (\mathbf{f} \langle \bar{p} \rangle^i) + \mathbf{m} \nabla^2 \bar{\mathbf{u}}_D \\ &+ \nabla \cdot (-\mathbf{r} \mathbf{f} \langle \bar{\mathbf{u}}' \bar{\mathbf{u}}' \rangle^i) - \left[ \frac{\mathbf{m} \mathbf{f}}{K} \bar{\mathbf{u}}_D + \frac{c_F \mathbf{f} \mathbf{r} \bar{\mathbf{u}}_D / \bar{\mathbf{u}}_D}{\sqrt{K}} \right] \end{aligned} \quad (2)$$

$$\mathbf{r} c_{pf} \left[ \frac{\partial \bar{T}_f}{\partial t} + \nabla \cdot (\bar{\mathbf{u}}_D \bar{T}_f) \right] = \nabla \cdot [k_f \nabla \bar{T}_f - \mathbf{r} c_{pf} \bar{\mathbf{u}}' \bar{T}'_f] \quad (3)$$

$$\begin{aligned} \mathbf{r} \nabla \cdot (\bar{\mathbf{u}}_D \langle k \rangle^i) &= \nabla \cdot \left[ \left( \mathbf{m} + \frac{\mathbf{m}_{t_f}}{\mathbf{s}_k} \right) \nabla (\mathbf{f} \langle k \rangle^i) \right] \\ &- \mathbf{r} \langle \bar{\mathbf{u}}' \bar{\mathbf{u}}' \rangle^i : \nabla \bar{\mathbf{u}}_D + c_k \mathbf{r} \frac{\mathbf{f} \langle k \rangle^i / \bar{\mathbf{u}}_D}{\sqrt{K}} - \mathbf{r} \mathbf{f} \langle \mathbf{e} \rangle^i \end{aligned} \quad (4)$$

$$\begin{aligned} \mathbf{r} \nabla \cdot (\bar{\mathbf{u}}_D \langle \mathbf{e} \rangle^i) &= \nabla \cdot \left[ \left( \mathbf{m} + \frac{\mathbf{m}_{t_f}}{\mathbf{s}_e} \right) \nabla (\mathbf{f} \langle \mathbf{e} \rangle^i) \right] \\ &+ c_{1e} (-\mathbf{r} \langle \bar{\mathbf{u}}' \bar{\mathbf{u}}' \rangle^i : \nabla \bar{\mathbf{u}}_D) \frac{\langle \mathbf{e} \rangle^i}{\langle k \rangle^i} + c_{2e} c_k \mathbf{r} \frac{\mathbf{f} \mathbf{e}_f / \bar{\mathbf{u}}_D}{\sqrt{K}} \\ &- c_{2e} f_e \mathbf{r} \mathbf{f} \frac{\langle \mathbf{e} \rangle^{i^2}}{\langle k \rangle^i} \end{aligned} \quad (5)$$

$$-\mathbf{r} \mathbf{f} \langle \bar{\mathbf{u}}' \bar{\mathbf{u}}' \rangle^i = \mathbf{m}_{t_f} \langle \bar{\mathbf{D}} \rangle^v - \frac{2}{3} \mathbf{f} \mathbf{r} \langle k \rangle^i \mathbf{I} \quad (6)$$

$$\mathbf{m}_{t_f} = \mathbf{r} c_m f_m \frac{\langle k \rangle^{i^2}}{\langle \mathbf{e} \rangle^i}, \quad (7)$$

## 2.1. Macroscopic non linear Reynolds stress:

In this work, results produced by non-linear eddy-viscosity models (NLEVM) are investigated. The macroscopic non-linear turbulence model here proposed is constituted by the same system of equations formerly given by Pedras and de Lemos (2001a). The sole difference between both macroscopic models (Linear and Non-Linear) lies in the expression for the macroscopic Reynolds stress, kept to second order, this new macroscopic non-linear stress-strain-rate equation can be rewritten in the form:

$$\begin{aligned} -\mathbf{f} \langle \bar{u}'_i \bar{u}'_j \rangle^i &= \left( \mu_{t_f} \langle \bar{D}_{ij} \rangle^v \right)^L - \left( c_{1NL} \mu_{t_f} \frac{\langle k \rangle^i}{\langle \mathbf{e} \rangle^i} \left[ \langle \bar{D}_{ik} \rangle^v \langle \bar{D}_{kj} \rangle^v - \frac{1}{3} \langle \bar{D}_{kl} \rangle^v \langle \bar{D}_{kl} \rangle^v d_{ij} \right] \right)^{NL1} \\ &- \left( c_{2NL} \mu_{t_f} \frac{\langle k \rangle^i}{\langle \mathbf{e} \rangle^i} \left[ \langle \bar{O}_{ik} \rangle^v \langle \bar{S}_{kj} \rangle^v + \langle \bar{O}_{jk} \rangle^v \langle \bar{S}_{ki} \rangle^v \right] \right)^{NL2} \\ &- \left( c_{3NL} \mu_{t_f} \frac{\langle k \rangle^i}{\langle \mathbf{e} \rangle^i} \left[ \langle \bar{O}_{ik} \rangle^v \langle \bar{O}_{jk} \rangle^v - \frac{1}{3} \langle \bar{O}_{lk} \rangle^v \langle \bar{O}_{lk} \rangle^v d_{ij} \right] \right)^{NL3} - \frac{2}{3} \mathbf{f} \mathbf{d}_{ij} \mathbf{r} \langle k \rangle \end{aligned} \quad (8)$$

where  $\mathbf{d}_{ij}$  is the Kronecker delta; the superscripts (*L* and *NL*) in the equation (8) indicate Linear and Non-Linear contributions,  $\mathbf{m}_{t_f}$  is the macroscopic turbulent viscosity,  $\langle \bar{D}_{ij} \rangle^v$  and  $\langle \bar{O}_{ij} \rangle^v$  are the deformation and vorticity tensors, written in the indexed form, respectively, as:

$$\langle \bar{D}_{ij} \rangle^v = \left( \frac{\partial \bar{u}_{i_D}}{\partial x_j} + \frac{\partial \bar{u}_{j_D}}{\partial x_i} \right), \quad \langle \bar{O}_{ij} \rangle^v = \left( \frac{\partial \bar{u}_{i_D}}{\partial x_j} - \frac{\partial \bar{u}_{j_D}}{\partial x_i} \right). \quad (9)$$

In this work the non-linear model proposed by Shih et al (1993) was used and has the following expressions:

$$c_m = \frac{2/3}{1.25 + s + 0.9\Omega}, c_{INL} = \frac{0.75}{c_m(1000 + s^3)}, c_{2NL} = \frac{3.8}{c_m(1000 + s^3)}, c_{3NL} = \frac{4.8}{c_m(1000 + s^3)},$$

$$\text{where, } s = \frac{\langle k \rangle^i}{\langle e \rangle^i} \sqrt{\frac{1}{2} \langle \bar{D}_{ij} \rangle^v \langle \bar{D}_{ij} \rangle^v} \text{ and } \Omega = \frac{\langle k \rangle^i}{\langle e \rangle^i} \sqrt{\frac{1}{2} \langle \bar{\Omega}_{ij} \rangle^v \langle \bar{\Omega}_{ij} \rangle^v} \quad (10)$$

Note that equation (6) is recovered if constants  $c_{INL}$ ,  $c_{2NL}$  and  $c_{3NL}$  in (8) are set to zero.

### 3. NUMERICAL METHOD AND RESULTS

The governing equations to simulate the turbulent flow and heat transfer inside a hybrid configuration were discretized using the finite volume procedure, (Patankar (1980)), applied to a boundary-fitted coordinate system. Classical wall function was employed to describe the flow near the wall. The calculation process starts with the solution of the two momentum equations. Next, the velocity field is adjusted in order to satisfy the continuity principle. This adjustment is obtained by solving the pressure correction equation (SIMPLE algorithm). After that, the turbulence model equations and the energy equation are relaxed to update the  $k$ ,  $e$  and temperature fields.

The geometry of the flow under consideration is shown in Figure 1. For this geometry the step height,  $H$ , was taken as 0.1 m. Results were obtained considering an inlet Reynolds number of  $Re = 132000$  based on the height of the step. Inlet boundary conditions are illustrated in Figure 1. An orthogonal mesh of size 360x60 was used. Preliminary results for unobstructed flow were obtained in order to assess the performance of the linear and non-linear turbulence models in clear domains. Numerical parameters for this cases were  $a = 0$ ,  $c_F = 0$ ,  $\phi = 1$  and  $K \rightarrow \infty$ . The working fluid is air ( $\rho = 1.15 \text{ [kg/m}^3\text{]}$ ,  $\mathbf{m} = 1.8 \times 10^{-5} \text{ [Ns/m}^2\text{]}$ ,  $Pr = 0.72$ ,  $c_{pf} = 1006.0 \text{ [J/Kg}^\circ\text{C}\text{]}$ ) with a uniform inlet temperature of  $T_{in} = 20^\circ\text{C}$ . The boundary conditions for the thermal field are constant heat flux ( $q_w = 3000 \text{ [W/m}^2\text{]}$ ) on the step wall, and  $q_w = 0$  on the other surfaces of the step and channel. The constant value for the turbulent Prandtl number was  $Pr_t = 0.9$ .

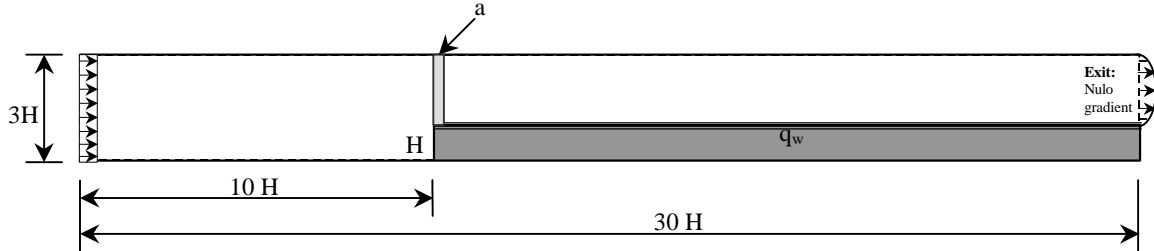


Figure 1. Problem geometry with porous insert: turbulent flow and heat transfer.

Table 1 shows the results for the pressure drop at channel with and without the porous material simulated by the linear (L\_HRN) and non linear (NL\_HRN) models. These quantities were obtained as:

$$\overline{\Delta p} = \frac{1}{A_t} \int_{A_t} (p_{in} - p_{ex}) dy \quad (11)$$

where the sub-indexes  $in$  and  $ex$  refer to the channel inlet and exit, respectively.

The results presented in Table 1 show an expressive gain in the pressure drop,  $\overline{\Delta p}$ , for the channel with porous insert as compared to the clean channel. The gain in the pressure drop is more pronounced as we decreased the permeability and increased the thickness of the porous material.

Table 1. Pressure drop in the channel with porous obstruction.

Turbulence models	Thickness a [m]	Porosity $\phi$	Permeability K [m <sup>2</sup> ]	Pressure drop $\bar{\Delta p}$ [N/m <sup>2</sup> ]	
L_HRN	0.0083	0.85	-	485.87	
			$10^{-2}$	620.50	
			$10^{-4}$	1413.44	
		0.95	$10^{-6}$	6892.93	
			$10^{-2}$	600.86	
		0.85	$10^{-4}$	1418.72	
	0.0163		$10^{-2}$	681.70	
			$10^{-4}$	1922.22	
			$10^{-6}$	12019.61	
	0.95	$10^{-2}$	658.27		
		$10^{-4}$	1924.42		
	0.0250	0.85	$10^{-2}$	735.08	
			$10^{-4}$	2426.36	
			$10^{-6}$	17104.30	
		0.95	$10^{-2}$	709.79	
			$10^{-4}$	2428.54	
NL_HRN	0.0083	0.85	-	486.91	
			$10^{-2}$	621.34	
			$10^{-4}$	1422.06	
		0.95	$10^{-6}$	6952.29	
			$10^{-2}$	601.38	
			$10^{-4}$	1420.50	
	0.0163	0.85	$10^{-2}$	682.65	
			$10^{-4}$	1933.78	
			$10^{-6}$	12103.35	
		0.95	$10^{-2}$	659.56	
			$10^{-4}$	1927.44	
		0.0250	$10^{-2}$	737.89	
			$10^{-4}$	2440.07	
			$10^{-6}$	17196.32	
			$10^{-2}$	709.91	
			$10^{-4}$	2432.63	

Figures 2-5 show distributions for the friction coefficient,  $C_f$  and for the Stanton number,  $St$ , along the heated surface of the step. These coefficients are given by:

$$C_f = \frac{t_w}{r U_0^2 / 2}, \quad St = \frac{q_w}{r c_{pf} U_0 (T_w - T_{in})} \quad (12)$$

Again one should note the expressive effect of the permeability on the calculated parameters. The distributions for both the  $St$  and the  $C_f$  follow the same path in regard to the sensitivity of the type of model used. Or say, both linear and non-linear models predict comparable results. It is interesting to emphasize that for the smallest thickness,  $a=0.083H$ , it's obtained the smallest picks of  $St$ , a feature that can be used to great advantage when optimizing engineering flows, besides introducing smaller load losses.

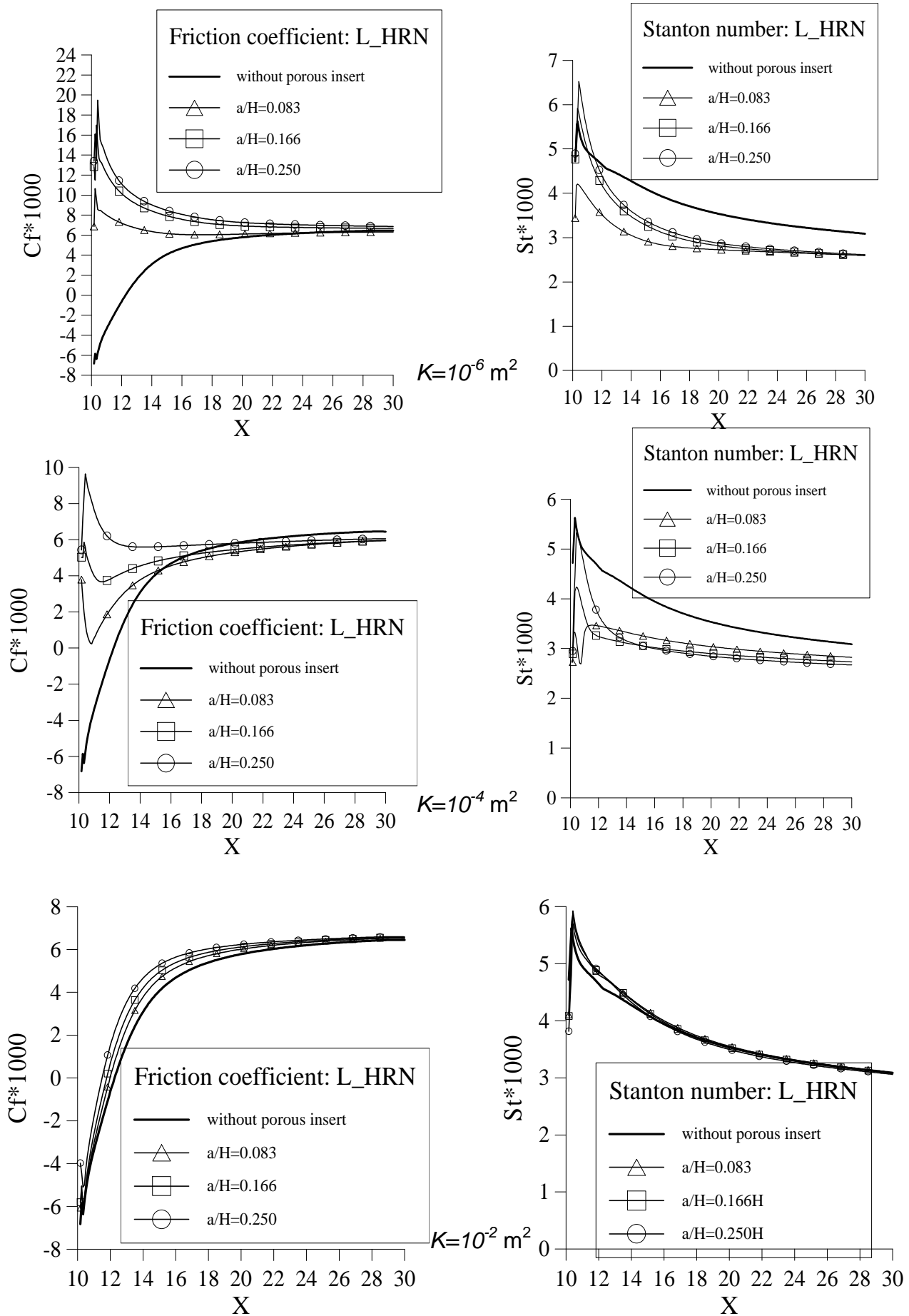


Figure 2. Friction coefficient and Stanton number distribution for  $\phi=0.85$  using the Linear model.

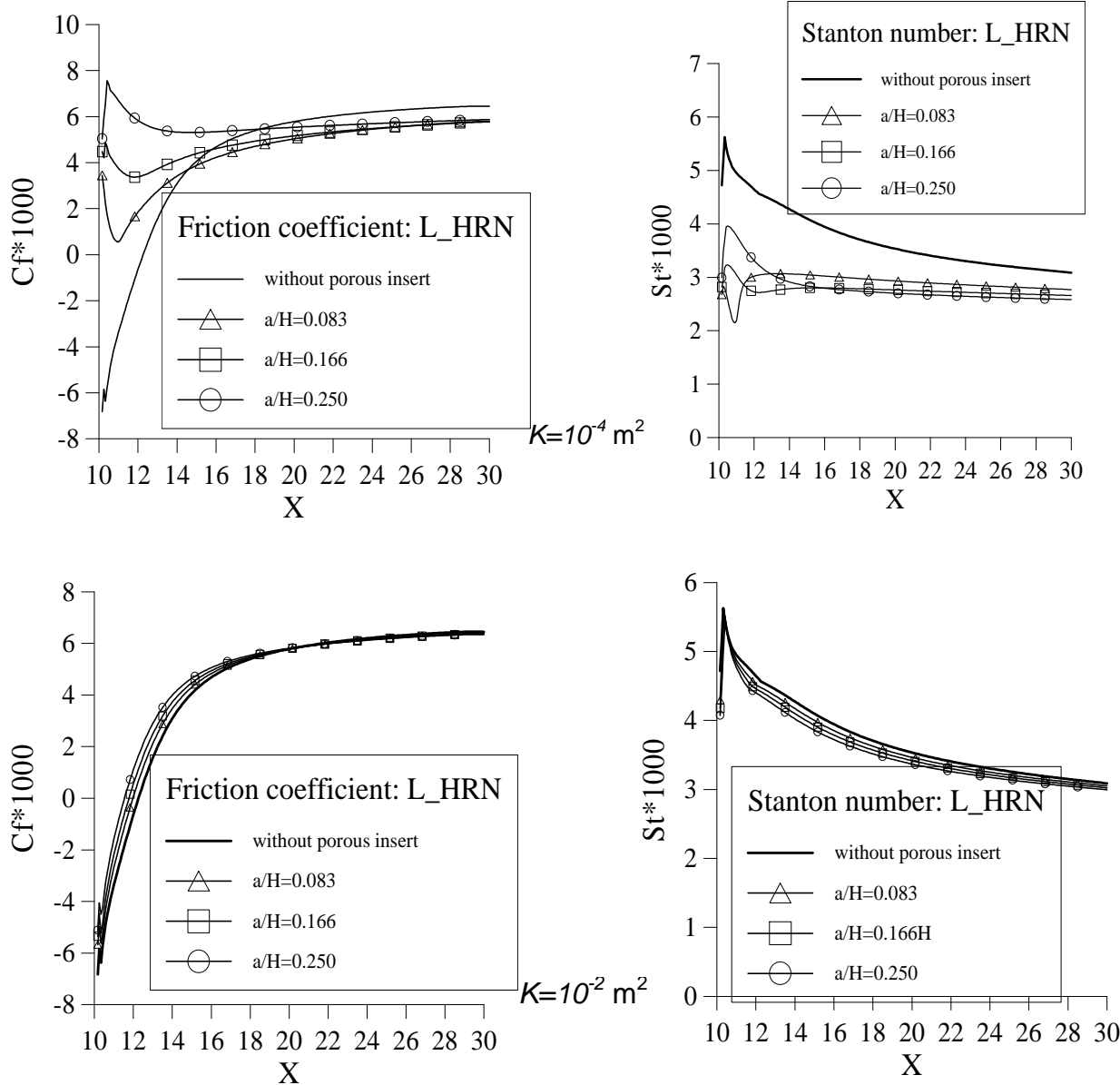


Figure 3. Friction coefficient and Stanton number distribution for  $\phi=0.95$  using the Linear model.

#### 4. CONCLUSION

In this work, the turbulence linear and non-linear models, using wall functions, were used to simulate convective heat transfer in a channel with a step. A porous material was placed in a flow passage and their parameters such as porosity  $f$ , permeability  $K$ , and thickness  $a$  of the porous insert were varied in order to analyze their effects on the flow pattern.

Results of friction coefficient ( $C_f$ ) and Stanton number ( $St$ ) distribution indicated that the permeability of the insert plays the dominant role in changing the final flow and heat transfer pattern rather than the porosity or thickness of the material. However, a decrease of the material permeability results in an expressive gain in the pressure drop, as observed in Table 1. It has been observed that using the smallest thickness,  $a=0.083H$ , it's obtained the smallest picks of  $St$ , besides introducing smaller load losses. Sometimes, for another thickness is not advantage to use the porous inserts, because the  $St$  picks becomes more intense than for the clean channel. A sudden increase of  $St$  around the reattachment point, known to be undesirable in many practical situations may be avoided by the use of a porous plate. Thus, in spite of porous insert to produce a resistance to the flow, which results in the form of a pressure loss in the downstream locations (see Table 1) requesting an increase in the pumping power to maintain the flow, the suppression of the recirculation bubble decreases the risk of a overheating on the surface, more specifically around the

reattachment point. Those findings may be used to advantage by design engineers when optimizing thermo-mechanical equipment.

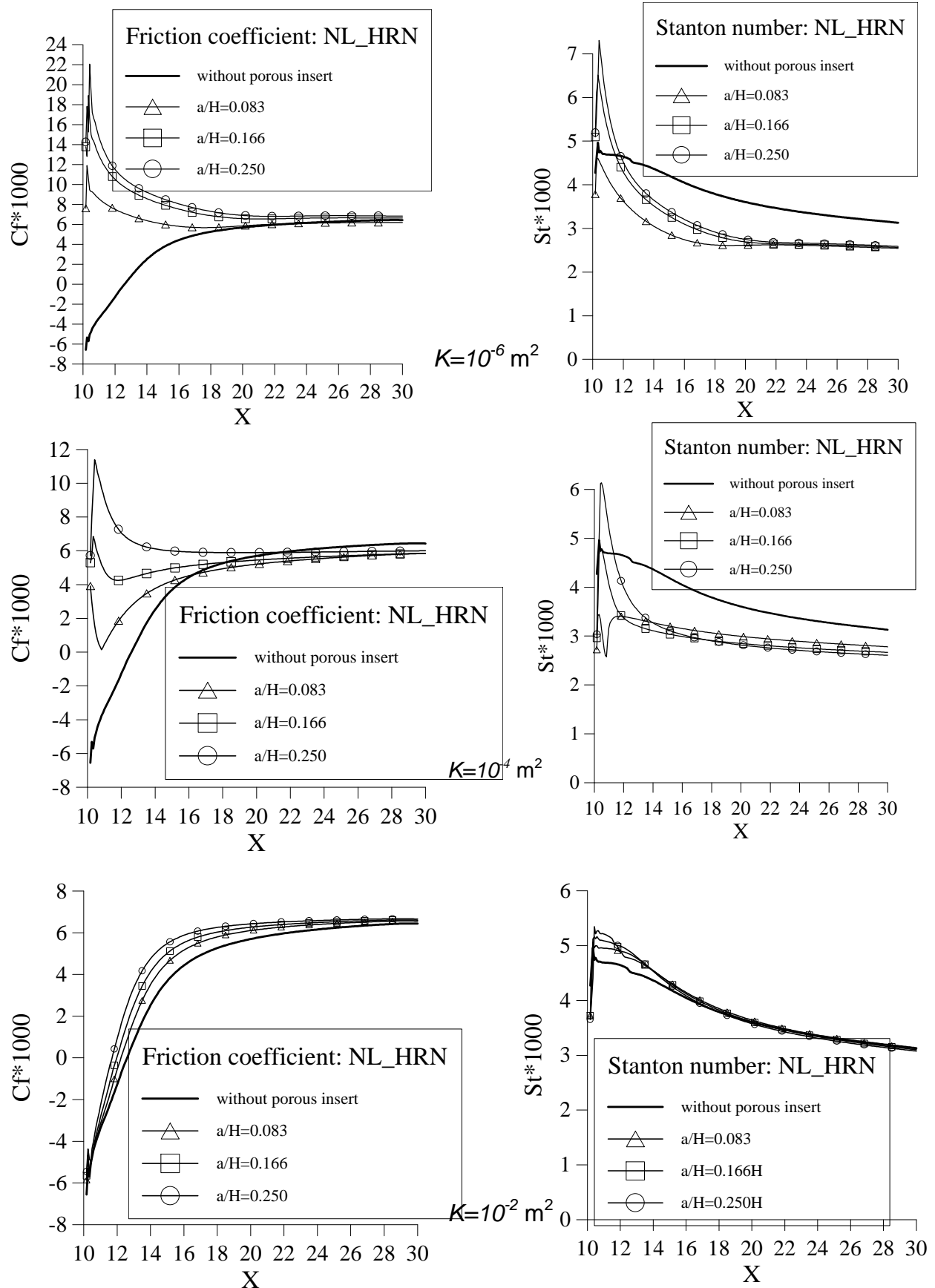


Figure 4. Friction coefficient and Stanton number distribution for  $\phi=0.85$  using the Non Linear model

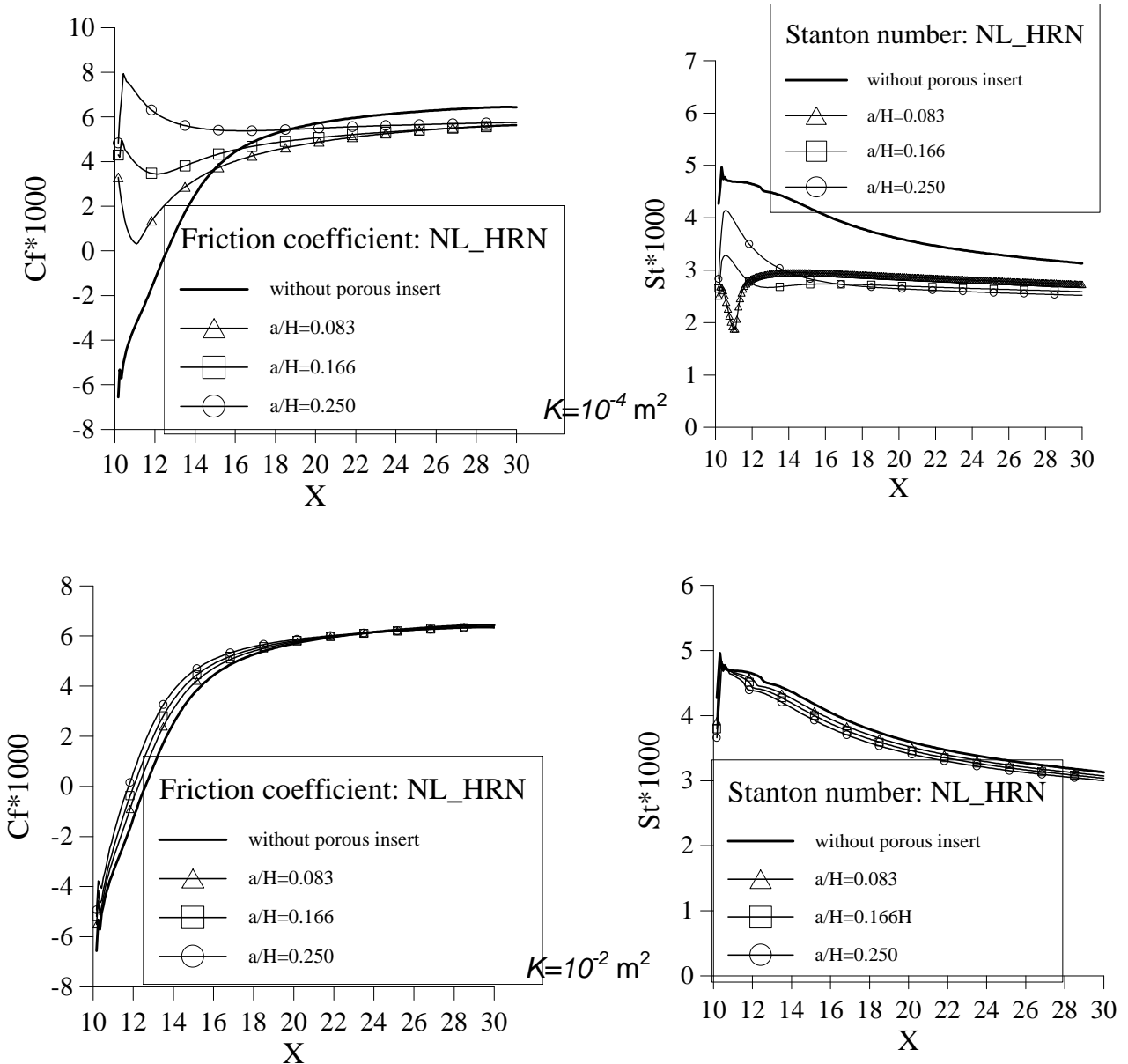


Figure 5. Friction coefficient and Stanton number distribution for  $\phi=0.95$  using the Non Linear model

## 5. ACKNOWLEDGMENTS

The authors would like to thank FAPESP and CNPq, Brazil, for their financial support during the preparation of this work.

## 6. REFERENCES

Assato, M. and de Lemos, M.J.S., 2000, "Tratamento Numérico e Aplicações de um Modelo de Viscosidade Turbulenta Não Linear para Alto e Baixo Reynolds", 2<sup>th</sup> ETT- Escola Brasileira de Primavera Transição e Turbulência, Uberlândia/MG, Brazil, Dez. 11-15.

Assato, M., Pedras, M.H.J. & de Lemos, M.J.S., 2002, "Numerical Solution of Turbulent Flow Past a Backward-Facing-Step With a Porous Insert Using Linear and Non-Linear  $k$ - $\epsilon$  Models", Proc. of APM2002 - 1st Inter. Conf. on Applications of Porous Media, Paper APM-163, V. CDROM, Eds. R. Bennacer and A.A. Mohamed, 2002. v.1. p.539 – 550, June 2-8, Jerba, Tunisia.

Assato, M. & de Lemos, M. J. S., 2003, "Heat Transfer in a Back-step Flow Past a Porous Insert using a Non-Linear Turbulence Model and a Low Reynolds Wall Treatment", In: 3<sup>rd</sup> International Conference on Computational Heat and Mass Transfer, Banff, Canada, May 26-30, Proc. 3rdICCHMT, University of Calgary.

Brinkman, H.C., 1948, "Calculations of the Flow of Heterogeneous Mixture Through Porous Media" Applied Science Research, 2, pp. 81-86.

Chan, E.C., Lien, F.S. and Yovanovich, M.M., 2000, "Macroscopic Numerical Study of Forced Convective Heat Transfer in a Back-step Channel Through Porous Layer", Proceedings of NTHC2000, ASME National Heat Transfer Conference, 20<sup>th</sup> –22<sup>th</sup> August, 2000, Pittsburgh, Pennsylvania, USA.

de Lemos, M.J.S. and Pedras, M.H.J., 2001, "Recent Mathematical Models for Turbulent Flow in Saturated Rigid Porous Media". ASME Journal of Fluids Engineering, vol. 123 (4), pp. 935-940.

Lumley, J.L., 1970, "Toward a Turbulent Constitutive Relation", J. Fluid Mech., 41, 413.

Nield, D.A. and Bejan, A., 1992, "Convection in Porous Media", Springer-Verlag.

Ochoa-Tapia, J. A.; Whitaker, S., 1995, "Momentum Transfer at the Boundary between a Porous Medium and a Homogeneous Fluid-I. Theoretical Development.", Int. J. Heat Mass Transfer, vol. 38, pp. 2635-2646.

Pedras, M. H. J. and de Lemos, M.J.S., 2001, "Macroscopic Turbulence Modeling for Incompressible Flow Through Undeformable Porous Media". Int. J. Heat Mass Transfer, vol. 44 (6), pp. 1081-1093.

Pedras, M.H.J. and de Lemos, M.J.S., 2001, "Simulation of Turbulent Flow in Porous Media Using a Spatially Periodic Array and a Low Re Two-Equation Closure". Numer. Heat Transfer Part A- Appl, vol. 39 (1), pp. 35-59.

Pedras, M. H. J. and de Lemos, M. J. S., 2001, "On Mathematical Description and Simulation of Turbulent Flow in a Porous Medium Formed by an Array of Elliptic Rods". ASME Journal of Fluids Engineering, vol. 123 (4), pp. 941-947.

Rivlin, R.S., 1957, "The Relation Between the Flow of Non-Newtonian Fluids and Turbulent Newtonian Fluids", Q. Appl. Maths, 15, 212.

Rocamora, Jr., F.D. and de Lemos, M.J.S., 2000, Heat Transfer in Suddenly Expanded Flow in a Channel with Porous Inserts", Proceedings of NTHC2000, ASME National Heat Transfer Conference, 20<sup>th</sup> –22<sup>th</sup> August, 2000, Pittsburgh, Pennsylvania, USA.

Shih, T.H., Zhu, J. and Lumley, J.L., 1993, "A Realizable Reynolds Stress Algebraic Equation Model", NASA TM-105993.

Speziale, C.G., 1987, "On Nonlinear  $k-l$  and  $k-\epsilon$  Models of Turbulence", J. Fluid Mech., vol. 176, pp. 459-475.

Patankar, S. V., 1980, "Numerical Heat Transfer and Fluid Flow", Hemisphere, New York.